

A passive all-optical semiconductor device for level amplitude stabilization based on fast saturable absorber

H. Trung Nguyen,^{1,a)} J.-L. Oudar,¹ S. Bouchoule,¹ G. Aubin,¹ and S. Sauvage²

¹Laboratoire de Photonique et de Nanostructures, CNRS-LPN, 91460 Marcoussis, France

²Institut d'Électronique Fondamentale, UMR8622, Université Paris XI, 91405 Orsay, France

(Received 10 November 2007; accepted 21 February 2008; published online 19 March 2008)

A high-speed saturable-absorber-based device (response time below 2.5 ps) providing a significant amplitude stabilization is demonstrated. The experimental results allow estimating that the amplitude fluctuations of the output should be reduced by about 90% compared to the input fluctuations, within the input power range of (5–18 $\mu\text{J}/\text{cm}^2$). This device has been studied in view of its possible use for bit-1 noise reduction. When combined with a state-of-art saturable absorber device, this could provide a simple and compact scheme for the complete reamplification and reshaping regeneration of digital optical signals. © 2008 American Institute of Physics.

[DOI: 10.1063/1.2899940]

Ultrafast all-optical switches are key devices for future optical-communication networks, owing to their capacity of extending the reach of high bit rate fiber links.^{1,2} Regeneration is necessary since the optical signal is degraded in the systems due to signal impairments from, e.g., loss, dispersion, noise, and crosstalk. All-optical reamplification and reshaping (2R) regeneration is used to improve the signal-to-noise ratio through extinction ratio improvement and amplitude noise reduction. These improvements can be achieved with devices which have a nonlinear transfer function (output power as a function of input power), which allows to make a decision between a logical one and zero.³ Several schemes of all-optical regenerators have been proposed based on the nonlinear effects in fiber such as nonlinear optical loop mirror,^{4,5} self-phase modulation induced spectral broadening and filtering,^{6,7} or similariton generation configuration.⁸ Semiconductor devices, such as semiconductor optical amplifier-based (SOA) interferometers⁹ and saturable absorbers (SA) can also be used. Among these, SA gates are particularly attractive, owing to their simplicity and their fully passive operation mode (no Peltier cooler and no bias voltage). Recent experiments using high repetition rate signals showed that, with the benefit of quantum wells having an ultrafast carrier recombination rate,^{10,11} SA microcavity devices are very promising devices for 2R regeneration at 160 Gbit/s.^{12,13}

Up to now, however, SAs actually have only been used to achieve an extinction ratio improvement, but this can only reduce the noise of logical zeros. The noise of logical ones (bit-1) is not reduced and can even be increased. In order to perform a complete regeneration, SAs have typically been used in combination with other devices that can provide the level stabilization at the bit time scale, thereby reducing the bit-1 noise. Fiber-based or SOA-based devices have recently been presented for such a purpose. However the fiber-based gates generally require strong input powers and they are not adequate for wavelength division multiplexing (WDM) applications.¹⁴ While SOAs are active elements, they have a

slow gain recovery time, furthermore, SOAs introduce more noise.¹⁵

In this letter, we propose and demonstrate a configuration of SA-based microcavity that can provide an amplitude stabilization, suggesting that this device can be used to achieve the required of bit-1 noise reduction. The advantage of this approach is to make a complete all-optical high bit rate 2R regeneration relying upon a single technology. The device is based on a simple variation of the well-known reflection-mode SA microcavity used for extinction ratio enhancement, with cavity parameters designed for obtaining a decreasing curve of reflectance versus input power, while an increasing curve is obtained with the usual design. Therefore, it can be used with similar multiquantum well (QW) structures, whose carrier lifetime can be reduced by introducing capture and recombination centers via low temperature epitaxy, high-energy ion implantation, Be or Fe doping.

The proposed microcavity consists of a Fabry-Pérot structure. As is well known, the cavity reflectance exhibits a dip at resonance. The minimum value of the cavity reflection coefficient at normal incidence can be expressed as

$$R_{\text{cav}} = \left| \frac{\sqrt{R_f} - \sqrt{R_b^{\text{eff}}}}{1 - \sqrt{R_f R_b^{\text{eff}}}} \right|^2. \quad (1)$$

In this equation, R_f and R_b are the front mirror and the back mirror reflectivity, respectively, and $R_b^{\text{eff}} = R_b e^{-2\eta N \Gamma}$ is the effective back mirror reflectivity, where η is the single-pass absorption per QW, N is number of QW, and Γ is the longitudinal confinement factor of the microcavity.¹⁶ We note that R_b^{eff} increases when the absorption decreases. Equation (1) shows that if $R_f > R_b^{\text{eff}}$ at low intensity, then the depth of the reflectance dip at resonance increases when the absorbing layer becomes more transparent at higher intensity. With this design, the device reflectance decreases with an increase of incident power, which can provide significant amplitude stabilization in reflected power output. We note that, in the plane wave approximation, the cavity reflectance may go to zero, for some critical intensity I_c such that $R_b^{\text{eff}}(I_c) = R_f$. This will occur when $R_b^{\text{eff}}(I_0 \approx 0) < R_f < (R_b^{\text{eff}})_{\text{max}}$, where $(R_b^{\text{eff}})_{\text{max}}$ is the value (approximately equal to R_b) of R_b^{eff} in the fully saturated case.

^{a)}Electronic mail: hoang-trung.nguyen@lpn.cnrs.fr. URL: <http://www.lpn.cnrs.fr>.

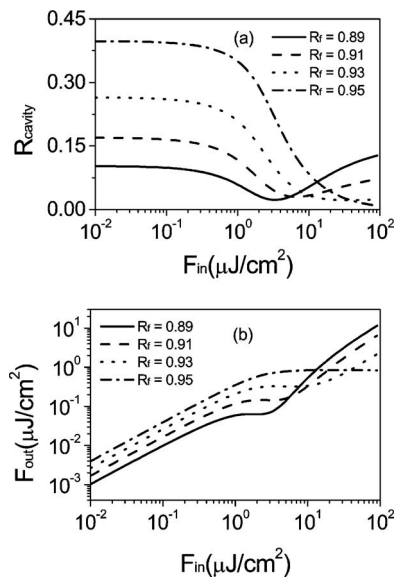


FIG. 1. Calculated nonlinear response of the investigated device for different values of the front mirror reflectivity R_f . (a) Microcavity reflectance curves vs input beam maximum fluence. (b) Output pulse fluence vs input fluence. In the simulated device, $R_b=0.945$ and $R_f=0.786$.

Numerical simulations of the nonlinear response of these devices have been developed using a steady state model. The absorption coefficient is assumed, as in a two-level system, to decrease linearly with carrier density n , i.e., $\eta(n) = \eta_0(1 - n/n_t)$, where n_t is the carrier density at transparency, assumed equal to $2 \cdot 10^{12} \text{ cm}^{-2}$ in the present calculation. The intracavity field enhancement in the microcavity is taken into account.¹⁶ In this calculation, the input beam was modeled with a Gaussian transverse intensity profile, to account for the inherent difference of the microcavity nonlinear response at the center and at the edges. Due to spatial averaging effects, the overall nonlinear response is smaller with a Gaussian spatial profile than with a uniform (flat-top) profile, resulting in an increased switching energy. Examples of calculated curves are displayed in Figs. 1(a) and 1(b). It is interesting to note that, due to the transverse profile nonuniformity, the microcavity reflectance does not go to zero for some input power, in contrast with the plane-wave situation. This is because R_b^{eff} is spatially varying due to the nonuniform absorption saturation, so it cannot be in perfect balance with R_f . The calculated curves of Fig. 1(b) show that a significant power stabilization can be obtained for a relatively wide range of R_f values. However, depending on the precise value of R_f , the maximum stabilization effect occurs at markedly different input powers.

In order to provide an experimental test of this concept, a device was designed, based on the results of the above numerical calculations. The fabricated device structure named MD7 includes an absorbing region made of $7x(\text{InGaAs}/\text{InAlAs})$ multiquantum wells, grown by metal-organic vapor-phase epitaxy upon an InP substrate and contained in a microcavity. The QWs are suitably located at the antinode of the intracavity intensity. In order to reduce the carrier lifetime, the QWs were irradiated by 12 MeV Ni^{6+} ions with a dose of $4 \cdot 10^{11} \text{ cm}^{-2}$. Pump-probe measurements at 1551 nm showed a response time of 2.5 ps. The back mirror was made by deposition of silver layer (with a calculated reflectivity of 0.945), while three pairs of $(\text{ZnS}/\text{YF}_3; \lambda/4; \lambda/4)$ were deposited as a top mirror with

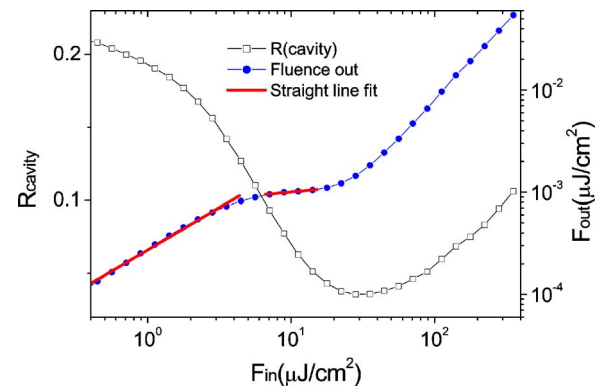


FIG. 2. (Color online) Experimental reflectance and input-output transfer function of the microcavity device. Straight line fits of some portions of the input-output data points (in log-log scale) are indicated, to show the device stabilization efficiency.

0.92 reflectivity. The sample was mounted on a Si substrate by Au-In bonding, to ease heat dissipation and limit thermo-optics effects.

To estimate the potential for noise reduction of this device, we measured its transfer function, i.e., the time-averaged output power versus input power. The experimental setup consists of a mode-locked fiber laser producing 1 ps pulses at 19.44 MHz, with wavelength adjustable in the range from 1545 to 1560 nm. The input signal, after passing through a variable attenuator, is focused onto the sample with a spot size of $3.1 \mu\text{m}$ (diameter at $1/e$ intensity) thanks to a microlensed fiber. The reflected signal was detected and analyzed by an optical spectrum analyzer. On Fig. 2 are displayed the microcavity reflectance and the reflected output power. As can be seen, the reflectance decreases with increasing input power. The input-output transfer function and the associated straight-line fit drawings (with slope 0.1) show that the relative amplitude fluctuation at the output would be reduced to 10% of the input relative fluctuation, in the input energy fluence range $5-18 \mu\text{J}/\text{cm}^2$. Thus, it should provide a significant amplitude stabilization of the reflected signal. In order to study the effect of changing the front mirror reflection coefficient R_f , we modified it by immersing the device in an index-matching fluid. For this, we replaced the microlensed fiber with a planar-ended fiber with an internal focusing taper, providing the same focussed spot size than with the initial fiber, but with the beam waist at the flat fiber end. The sample was then mounted at the end of this fiber, thanks to a fluid matching the refractive index of the fiber. The experimental and calculated reflectance and input-output transfer curves are displayed in Figs. 3(a) and 3(b). In the case labeled MD7air, the microlensed fiber was used, with some air gap between the curved fiber end and the device. In the case labeled MD7liq, the thin liquid layer of refractive index $n=1.47$ reduces R_f to the value of 0.88. As shown on Fig. 3, a good agreement is obtained between the calculated and experimental results for incident fluences up to $20 \mu\text{J}/\text{cm}^2$. The disagreement observed at higher fluence may be attributed to the occurrence of thermo-optic effects,¹⁷ not included in the calculation. Furthermore, from the data displayed on Fig. 3(b) it can be seen that a variation of R_f from 0.92 to 0.88 induces a 6 dB decrease of the input power needed to obtain a stabilized reflected power. However, this improvement is obtained at the expense of a 4.3 dB increase of the device insertion loss.

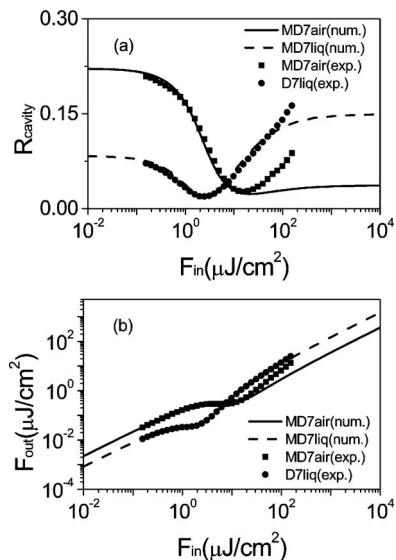


FIG. 3. Comparison of calculated and experimental results of (a) reflectance function and (b) output-input transfer function for the same structure MD7, with two different incident media, air and liquid, inducing a change of front mirror reflectivity.

As previously discussed, the present device could in principle be associated with a conventional SA device for bit-0 noise reduction, so as to make a complete 2R regenerator. Indeed, the fluence needed for amplitude stabilization with the present device is compatible with the saturation energy of a typical SA device used for bit-0 noise reduction.¹⁶ However, some critical issues should be considered, such as the possible adverse effect of one device on the functionality of the other device, and the fact that the device insertion loss needs to be compensated by some reamplification. We note that with already demonstrated complete 2R regeneration an additional amplifier is required.¹⁸ In order to fully assess the real potential of this approach, an experimental study of noise reduction involving the two devices subject to bit pattern sequences would be interesting, but it is beyond the scope of this letter.

In conclusion, we have demonstrated a high-speed saturable-absorber-based device that can provide a signifi-

cant amplitude stabilization of the bit-1 level of digital optical signals. A amplitude stabilization range of 5–18 $\mu\text{J}/\text{cm}^2$ has been measured. It shows that this device could be associated with a typical SA used for bit-0 to make a complete 2R regenerator. This device is thus promising for applications to all-optical 2R regeneration at ultrahigh bit rate.

We gratefully thank M. Van der Keur of Yenista Optics for the loan of the special focussing fibers used in the present work and also thank X. Lafosse for the dielectric deposition. This work was partly supported by the ANR-Telecom project FUTUR.

- ¹O. Leclerc, B. Lavigne, E. Balmefrezol, P. Brindel, L. Pierre, D. Rouvillain, and F. Seguineau, *J. Lightwave Technol.* **21**, 2779 (2003).
- ²O. Wada, *Chem.-Ing.-Tech.* **6**, 1 (2004).
- ³P. Ohlen and E. Berglind, *IEEE Photonics Technol. Lett.* **9**, 1011 (1997).
- ⁴J. Lucek and K. Smith, *Opt. Lett.* **18**, 1226 (1993).
- ⁵A. Bogoni, P. Ghelfi, M. Scaffardi, and L. Potti, *IEEE J. Quantum Electron.* **10**, 192 (2004).
- ⁶P. Mamyshev, ECOC'98, Madrid, Spain, 1998 (unpublished), Vol. 1, p. 475.
- ⁷A. G. Striegler and B. Schmauss, *J. Lightwave Technol.* **24**, 2835 (2006).
- ⁸C. Finot, S. Pitos, and G. Millot, *Opt. Lett.* **30**, 1776 (2005).
- ⁹J. Leuthold, L. Moller, J. Jacques, L. Z. S. Cabot, L. Zhang, P. Bernasconi, M. Cappuzzo, L. Gomez, E. Laskowski, E. Chen, A. Wong-Foy, and A. Griffin *Electron. Lett.* **40**, 554 (2004).
- ¹⁰E. L. Delpon, J. L. Oudar, N. Bouché, R. Raj, A. Shen, N. Stelmakh, and J. M. Lourtioz, *Appl. Phys. Lett.* **72**, 759 (1998).
- ¹¹J. Mangeney, H. Choumane, G. Patriarche, G. Leroux, G. Aubin, J. C. Harmand, J. L. Oudar, and H. Bernas, *Appl. Phys. Lett.* **79**, 2722 (2001).
- ¹²D. Massoubre, J. L. Oudar, J. Fatome, S. Pitois, G. Millot, J. Decobert, and J. Landreau, *Opt. Lett.* **31**, 537 (2006).
- ¹³J. Fatome, S. Pitois, A. Kamagate, G. Millot, D. Massoubre, and J.-L. Oudar, *IEEE Photonics Technol. Lett.* **19**, 245 (2007).
- ¹⁴L. Bramerie, Q. Le, S. Lobo, M. Gay, A. P. M. Joindot, J.-C. Simon, A. Poudoulec, M. Van der Keur, C. Devemy, D. Massoubre, J.-L. Oudar, G. Aubin, J. Dion, A. Shen, and J. Decobert, in Post-deadline paper in OFC2007, Anaheim, CA, USA, 2007 (unpublished).
- ¹⁵M. Gay, L. Bramerie, D. Massoubre, A. O'Hare, A. Shen, J. Oudar, and J. Simon, *IEEE Photonics Technol. Lett.* **18**, 1273 (2006).
- ¹⁶D. Massoubre, J.-L. Oudar, J. Dion, J.-C. Harmand, A. Shen, J. Landreau, and J. Decobert, *Appl. Phys. Lett.* **88**, 153513 (2006).
- ¹⁷D. Massoubre, J.-L. Oudar, A. O'Hare, M. Gay, L. Bramerie, J.-C. Simon, A. Shen, and J. Decobert, *J. Lightwave Technol.* **24**, 3400 (2006).
- ¹⁸D. Rouvillain, P. Brindel, E. Segueineau, L. Pierre, O. Leclerc, H. Choumane, G. Aubin, and J. Oudar, *Electron. Lett.* **38**, 1113 (2002).